S. Stifter and J. Lenarčič (eds.)

Advances in Robot Kinematics

With Emphasis on Symbolic Computation

Springer-Verlag Wien New York

MULTI-POINT COMPLIANCE CONTROL FOR REDUNDANT MANIPULATORS

Toshio Tsuji, Toshiaki Takahashi and Koji Ito

Faculty of Engineering, Hiroshima University,

Saijo-cho, Higashi-Hiroshima 724, Japan

Abstract. *The present paper proposes a new method called multi-point compliance control utilizing kinematic redundancy of the manipulators. The multi-point compliance control can regulate the compliance of several points on the manipulator's links as well as the end-point compliance. We define those points on the manipulator's links as virtual end-points, and derive the joint compliance which is able to control the virtual end-point compliance. It is shown that controlling the virtual end-point compliance is useful for certain environments where some obstacles impose restrictions on the task space of the manipulator.*

INTRODUCTION

Compliance control is one of the most effective control methods for the manipulators in contact with their environments, which can regulate compliance or stiffness of the end-point motion of the manipulators according to the tasks. Up to the present, several compliance control methods have been proposed (for example, *Salisbury, 1980: Kankaanranta and Koivo, 1988*). Especially, the active stiffness control proposed by *Salisbury (1980)* can determine the joint servo gains so as to achieve a desired end-point stiffness of the manipulator with redundant joint degrees of freedom. All of them, however, consider to regulate only the end-point compliance of the manipulators. In contrast to them, the present paper argues that kinematic redundancy of the manipulators should be positively utilized in terms of the compliance control.

Utilizing redundancy, the manipulator can perform subtasks while controlling the end-point compliance(*Tsuji, Ito and Nagaoka, 1990*). In the present paper, we consider a compliance regulation of several points on the manipulator's links as a subtask of the end-point compliance control. For example, when a manipulator close to obstacles performs a task which requires the end-point's compliant motion, it is required to avoid a collision with the obstacles as well as regulating the end-point compliance for the given task. In this case, we define a virtual end-point as the closest point on the manipulator to the obstacle. Then the compliances of the virtual end-points are regulated to avoid a collision in addition to the actual end-point compliance of the manipulator. We call this kind of compliance control *multi-point compliance control* , and discuss how to specify joint servo gains to achieve, as closely as possible, the desired multiple end-points compliance. The manipulator loses redundant joint degrees of freedom as the

number of the virtual end-points is increased, and finally becomes over-constrained. The method presented here can give the optimal solution for both the redundant and over-constrained cases and can assign order of priority to each end-point according to the given task.

VIRTUAL ARMS AND VIRTUAL END-POINTS

We consider a multi-joint manipulator having m joints shown in Fig.1(a). Since the manipulator performing a task which requires end-point's compliant motion is close to some obstacles, the manipulator may collide with them due to unexpected disturbance forces. Then, as shown in Fig.1(b), we define the virtual arm as an arm, the end-point of which is located at the closest point on the manipulator to a obstacle. Using the virtual arms, the interaction between the manipulator and its environment can be considered within the framework of compliance control. For example, to avoid a collision with the obstacles due to disturbance forces, the compliances of the virtual end-points should be as small (stiff) as possible in the direction of the obstacles.

Let the position vectors in the joint coordinate and the task coordinate be denoted as $\theta \in R^m$ and $X \in R^l$ respectively. Let also the corresponding force vectors be denoted as $\tau \in R^m$ and $F \in R^l$ where m and l are the dimensions of the joint and task coordinates. For redundant manipulators, m is larger than l.

When an external force F is applied to the end-point of the manipulator(in the following, we call it the actual arm in contrast to the virtual arm), we define compliance matrices as

$$dX = C_e F, \qquad (1)$$

$$d\theta = C_j \tau, \qquad (2)$$

where $dX = X - X^e$ and $d\theta = \theta - \theta^e$, X^e and θ^e are

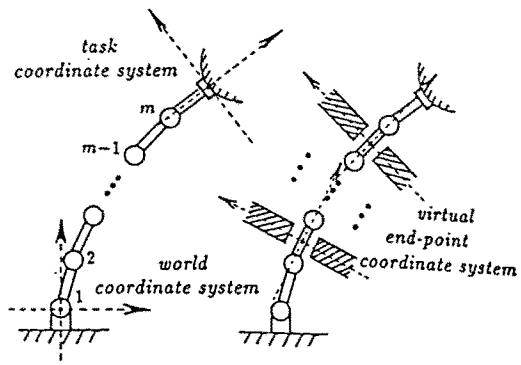

(a) manipulator close to obstacles

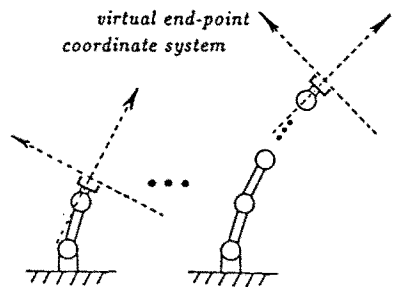

(b) virtual arms

Fig.1 Actual arm and virtual arms.

equilibrium points of the corresponding vectors. $C_e \in R^{l\times l}$ and $C_j \in R^{m\times m}$ are the end-point and joint compliance matrices of the actual arm respectively. Using the Jacobian matrix $J_0 \in R^{l\times m}$ relating the joint angle displacements to the end-point displacements in the world coordinate system, we can obtain

$$C_e = R_0 J_0 C_j {J_0}^T {R_0}^T, \tag{3}$$

where $R_0 \in R^{l\times l}$ is a rotation matrix from the world coordinate system to the task coordinate system. The above equation gives the kinematic relationship between the joint compliance matrix and the actual end-point compliance matrix.

The kinematic relationships between the joint compliance matrix and the virtual end-point compliance matrices can be derived in the same way. Let the virtual end-point compliance matrix of the i-th virtual arm be denoted as $C_{vi} \in R^{l\times l}$ $(i=1,2,\cdots,n-1)$, we can obtain

$$C_{vi} = R_i J_i C_j {J_i}^T {R_i}^T, \tag{4}$$

where $J_i \in R^{l\times m}$ is the Jacobian matrix relating the joint angle displacements to the i-th virtual end-point displacements, and $R_i \in R^{l\times l}$ is a rotation matrix from the world coordinate system to the virtual end-point coordinate system.

We concatenate the actual and virtual end-point compliance matrices, so that we can simultaneously express the compliance relationships for all end-points. The new equation is given by

$$C = J C_j J^T, \tag{5}$$

where $C \in R^{ln\times ln}$ is a concatenated compliance matrix, and $J \in R^{ln\times m}$ is a concatenated Jacobian matrix,

$$C = \begin{bmatrix} C_e & & & \\ & C_{v1} & & 0 \\ & & \ddots & \\ & 0 & & C_{vn-1} \end{bmatrix}, \quad J = \begin{bmatrix} R_0 J_0 \\ R_1 J_1 \\ \vdots \\ R_{n-1} J_{n-1} \end{bmatrix}. \tag{6}$$

It can be seen that finding the joint compliance matrix C_j which satisfies (5) can achieve the compliances of the actual and virtual arms simultaneously.

MULTI-POINT COMPLIANCE CONTROL

Now, let's assume that the desired end-point compliance matrices are given according to a task of the actual end-point and subtasks of the virtual end-points. We wish to solve the compliance kinematic equation (5) for the joint compliance matrix C_j.

Depending on the location of the virtual end-points, the matrix equation (5) may occur to be under-constrained, over-constrained or singular. Fig.2 shows the three cases. The actual arm is a seven-link planar arm (m=7), and the

dimension of the task space (l=3) includes two translations and one rotation. Locating a virtual end-point on the fourth link as shown in Fig.2(a), the desired concatenated compliance matrix C^* in (6) has 6 diagonal elements. Therefore, the matrix equation (5) is under-constrained and the concatenated Jacobian matrix J is of full row rank, as long as the actual arm is not in singular configurations. In Fig.2(b), five virtual arms are located. Since the desired concatenated compliance matrix has 18 diagonal elements, the manipulator is over-constrained. The concatenated Jacobian matrix J is of full column rank, and any joint compliance matrix C_j does not satisfy (5). On the other hand, Fig.2(c) shows a virtual arm which has its end-point on the sixth link. At first sight, the manipulator seems to be under-constrained. In this case, however, since there is only one joint between the actual and virtual end-points, it is impossible to regulate the end-point compliances of both the actual and virtual arms at the same time. The concatenated Jacobian matrix J is not of full rank. Consequently, the rank of the concatenated Jacobian matrix dominates the matrix equation (5).

Maximum rank decomposition of the concatenated Jacobian matrix J gives us an unified approach to all three cases.

$$J = J_a J_b , \tag{7}$$

where $J_a \in R^{l \times p}$ and $J_b \in R^{p \times m}$ have the same rank as J ; rank$J$ = rankJ_a = rankJ_b = p. Substituting (7) into (5), we can see

$$C = J_a J_b C_j {J_b}^T {J_a}^T . \tag{8}$$

The matrices J_a and J_b express an over-constrained part and an under-constrained part of the concatenated Jacobian matrix J, respectively.

To derive a general solution of the matrix equation (8), we should solve it for a matrix $J_b C_j {J_b}^T$ as the first step. Setting

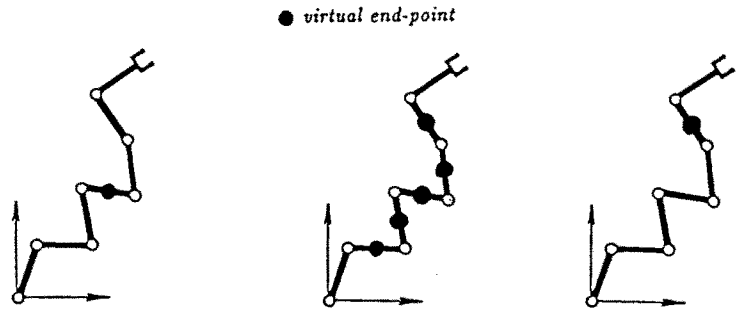

(a) an under-constrained case (b) an over-constrained case (c) a singular case

Fig.2 Three cases of the virtual arms.

$$C_{jb} = J_b C_j J_b^T , \tag{9}$$

we have

$$C = J_a C_{jb} J_a^T . \tag{10}$$

In general, since the matrix J_a is of full column rank, the solution C_{jb} which satisfies (10) does not exist. In this case, the goal is to find a matrix C_{jb} to minimize

$$G(C_{jb}) = || W(C^* - C) W^T || = || W(C^* - J_a C_{jb} J_a^T) W^T || , \tag{11}$$

where C^* is a desired concatenated compliance matrix. $||A||$ stands for matrix norm defined by

$$||A|| = \{ tr[A^T A] \}^{1/2}, \tag{12}$$

where $tr[A^T A]$ denotes a trace of matrix $A^T A$. The weighting matrix $W \in R^{ln \times ln}$ in (11) is a nonsingular diagonal matrix, which can assign order of priority to each end-point according to the given task.

The necessary condition that the optimal solution must satisfy is

$$\partial G(C_{jb}) / \partial C_{jb} = 0 . \tag{13}$$

Substituting (11) into (13) and expanding it, we obtain

$$C_{jb} = (WJ_a)^{\#} W C^* W^T \{ (WJ_a)^{\#} \}^T \tag{14}$$

$$(WJ_a)^{\#} = \{ (WJ_a)^T W J_a \}^{-1} (WJ_a)^T , \tag{15}$$

using the partial differential formulas about trace of matrix (*Athans, 1967*). This solution C_{jb} gives the end-point compliance matrix C which is the closest one to the desired compliance matrix C^* in terms of the cost function (11).

The second step is to solve (9) for the joint compliance matrix C_j using the matrix C_{jb}. Since the matrix J_b is of full row rank, the solution C_j which satisfies (9) always exists. Using the Moore-Penrose generalized inverse of J_b, we obtain the general solution (*Tsuji, Ito and Nagaoka, 1990*),

$$C_j = J_b^+ C_{jb} (J_b^T)^+ + [Z - J_b^+ J_b Z (J_b^+ J_b)^T] , \tag{16}$$

where $J_b^+ = J_b^T (J_b J_b^T)^{-1} \in R^{m \times p}$ and $Z \in R^{m \times m}$ is an arbitrary constant matrix. The matrix Z may be utilized in the other kind of subtasks.

Consequently, we can get the optimal joint compliance C_j using (14) and (16). The method presented here can be applied to all the cases shown in Fig.2. In the under-constrained cases, since $J_a = I_{ln}$ (a $ln \times ln$ unit matrix) and $J_b = J$, we can see $C_{jb} = C^*$. From (16), the joint compliance matrix is given by

$$C_j = J^+ C^* (J^T)^+ + [Z - J^+ J Z (J^+ J)^T] . \tag{17}$$

On the other hand, in the over-constrained cases, since $J_a = J$ and $J_b = I_m$, we can see $C_{jb} = C_j$. From (14), the joint compliance matrix is given by

$$C_j = (WJ)^{\#} W C^* W^T \{ (WJ)^{\#} \}^T . \tag{18}$$

Obviously, we can use (14) and (16) in the singular cases.

APPLICATION TO OBSTACLE AVOIDANCE

The multi-point compliance control is applied to an obstacle avoidance problem using a six-link planar manipulator as shown in Fig.3.

The manipulator is needed to perform a task which requires its end-point to be soft in the direction of x axis ($0.05m/N$) and to be stiff in the direction of y axis and its rotation ($0.01m/N$ and $0.01\ rad/N$, respectively) in the task coordinate system. And the third link of the manipulator lies between a couple of obstacles. A virtual end-point is located on a middle point of the third link. To avoid a collision with the obstacles, we wish to regulate the virtual end-point compliance to be stiff in the direction of y_{v1} axis and its rotation ($0.01\ m/N$ and $0.01\ rad/N$, respectively), while satisfying the desired end-point compliance of the actual arm. As a result, the desired concatenated compliance matrix C^* is given by

$$C^* = diag.[0.05, 0.01, 0.01, 0.05, 0.01, 0.01] .$$

In this case, the dimension of the desired compliance matrix is the same number as joints of the actual arm. Therefore, the concatenated Jacobian matrix J is square and nonsingular.

A simulation experiment was performed using the PD control,

$$\tau = K_j d\theta + B_j \dot{\theta} , \quad (19)$$

where $K_j \in R^{m\times m}$ is a position feedback gain given as an inverse of the joint compliance matrix C_j and, $B_j \in R^{m\times m}$ is a nonsingular velocity feedback gain. We used the Appel method for the manipulator dynamics (*Potknjak and Vukobratovic, 1978*) and the link parameters of the manipulator are shown in Table 1.

Fig.4 shows a response of the manipulator under the multi-point compliance control, where the disturbance force, f=$[-20, -20, 0]^T(N)$ in terms of the task coordinate

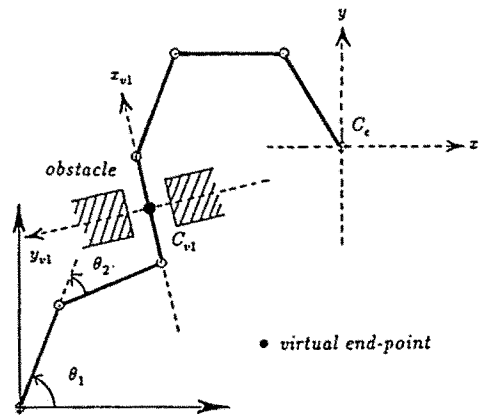

θ = [1.2, −0.8, 1.4, −0.6, −1.2, −1.0]^T (*RAD*)

Fig.3 A six-link planar manipulator close to the obstacles (a non-singular case).

Table 1 Link parameters.

	Link i (i=1, · · · ,6)
length(m)	0.2
mass(kg)	1.57
center of mass(m)	0.1
moment of inertia($kg \cdot m^2$)	10.0

system, is exerted to the actual end-point. The responses of the actual and virtual end-points are shown in Fig.4(b) and (c), respectively.

On the other hand, Fig.5 shows a simulation result under the active stiffness control(*Salisbury, 1980*) with the same condition as Fig.4, where the desired end-point compliance cannot include the virtual end-point one. The response of the actual end-point is almost same between Fig.4 and Fig.5. In terms of the virtual end-point, however, the effect of the multi-point compliance control appears clearly. In the active stiffness control, the large virtual end-point displacements for the disturbance force occur in the direction of the obstacle as

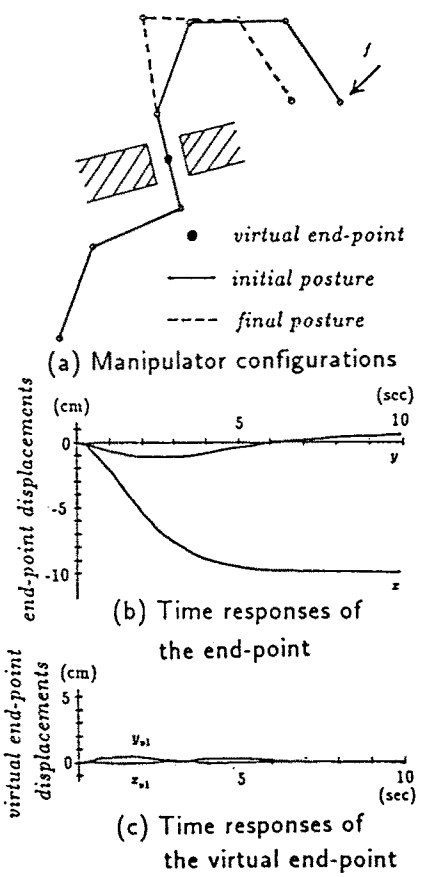

Fig.4 A motion profile for disturbance force under the multi-point compliance control.

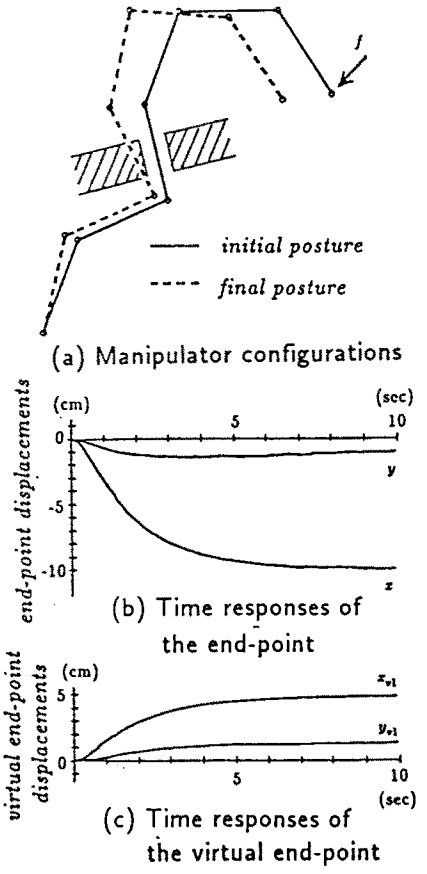

Fig.5 A motion profile for disturbance force under the active stiffness control.

shown in Fig.5. Since the multi-point compliance control can regulate the virtual end-point compliance, the virtual end-point displacements are very small as shown in Fig.4. It can be seen that the multi-point compliance control can regulate the configuration of the manipulator for any external force through the virtual end-point compliances. Therefore it is effective for the compliance control of the manipulator close to the obstacles.

CONCLUSION

In this paper, we proposed the multi-point compliance control method which was able to regulate the compliance of several points on the manipulator's links as well as the end-point compliance utilizing kinematic redundancy. The method can be applied to all kinematic conditions of the manipulator including the redundant, over-constrained and singular cases, and can give the joint servo gains to achieve, as closely as possible, the desired multiple end-point compliances. It is useful for certain environments where some obstacles impose restrictions on the task space of manipulators, such as many chemical plants.

Future research will be directed to extend the multi-point compliance control to the case where the end-point is mechanically constrained by the task environments. In that case, the virtual end-point compliance is determined not only by the joint compliance of the corresponding virtual arm expressed in (5) but also by the other joint compliance and the object compliance. As a result, the manipulator must be considered as a parallel link structure. This also leads to a development of the compliance control of the multi-fingered robotic hands and the multiple robot arms.

REFERENCES

Athans, M. (1967). The matrix minimum principle. *Information and Control, 11* , 592-606.

Kankaanranta, R. K. and Koivo, H. N. (1988). Dynamics and simulation of compliant motion of a manipulator. *IEEE J. of Robotics and Automation, 4, 2* , 163-173.

Potknjak, V. and Vukobratovic, M. (1987). Two new methods for computer forming of dynamic equation of active mechanisms. *Mechanism and Machine Theory, 14, 3* , 189-200.

Salisbury, J. K. (1980). Active stiffness control of a manipulator in Cartesian coordinates. *Proc.19th IEEE Conference on Decision and Control* ,95-100.

Tsuji, T., Ito, K. and Nagaoka, H. (1990). Identification and regulation of mechanical impedance for force control of robot manipulators. *11th IFAC World Congress* (to be appeared).